International Journal of Rotating Machinery
1999, Vol. 5, No. 4, pp. 283–293
Reprints available directly from the publisher
Photocopying permitted by license only

Dynamic Analysis of Engine Bearings*

H. HIRANI[a,†], K. ATHRE[a] and S. BISWAS[b]

[a] *Department of Mechanical Engineering,* [b] *Industrial Tribology, Machine Dynamics and Maintenance Engineering Centre, Indian Institute of Technology Delhi, Hauz Khas, New Delhi – 110 016, India*

(Received 23 April 1998; In final form 7 July 1998)

This paper presents a simple methodology to evaluate the stiffness and damping coefficients of an engine bearing over a load cycle. A rapid technique is used to determine the shaft 'limit cycle' under engine dynamic loads. The proposed theoretical model is based on short and long bearing approximations. The results obtained by present approximation are compared with those obtained by numerical method. The influence of thermal effects on the stiffness and damping coefficients is predicted by using a simplified thermal analysis. In order to illustrate the application of the proposed scheme, one engine main bearing and a connecting rod bearing are analysed.

Keywords: Non-linear analysis, Thermal effects, Dynamically loaded bearings, Dynamic coefficients, Engine bearing dynamics

1. INTRODUCTION

The most convenient way to analyse a complete system is to divide it into separate sub-systems or sub-structures (Parszewski, 1989), analyse each sub-system individually with less time-consuming methods, and then assemble into the whole system. In the present paper the journal bearing is treated as a sub-system of internal-combustion engine, and a semi-analytical method is proposed to evaluate dynamic characteristics of such a journal bearing subjected to dynamic load.

The principal bearings in internal combustion engines support the large dynamic loads. The gas force due to combustion/compression pressure in the engine cylinder and inertia forces due to reciprocating and unbalanced rotating masses contribute to the engine bearing loads. These loads vary markedly during a cycle of the crankshaft rotation. Under such dynamic loads, the behaviour of the rotor–bearing system becomes non-linear and to study rotor–bearing dynamics a complete non-linear transient simulation is used. Such an analysis involves the simultaneous solutions of dynamic Reynolds equation and equations of motion, for locating the journal centre at each time step.

The numerical solutions (Goenka, 1984; Roshan *et al.*, 1987) for solving coupled Reynolds equation

* This paper was originally presented at ISROMAC-7.
† Corresponding author. Fax: 91-11-6862037, -6857753. E-mail: harish@mech.iitd.ernet.in.

and equations of motion involve many iterations and are expensive in skill and time. The other analyses (Booker, 1971; Ritchie, 1975) make use of some closed form approximate solution to the dynamic Reynolds equation for reducing computation time. The authors have reported recently a rapid method for analysis of dynamically loaded journal bearings (Hirani *et al.*, 1998), wherein analytical pressure expression was proposed to eliminate the need of time-consuming and tedious iterations for pressure calculations. A two-dimensional non-linear root finding Newton–Raphson method with globally converging strategy was applied to evaluate the velocity of rotor-centre at each time step. The journal displacement at next time step was determined by using Runga–Kutta method. The results obtained match well with those using FEM (Goenka, 1984) at much less computation cost.

The knowledge of hydrodynamic damping and elastic properties of the journal bearing is desirable for accurate determination of the critical speeds of crankshaft and for the anticipation of its behaviour in the neighbourhood of such speeds. Moreover, it is very important to examine how dynamic coefficients vary in a crankshaft cycle. If this could be observed, it would be useful for analysis of engine vibrations. Unfortunately, the constant values of stiffness and damping coefficients have received more attention, and variation in these coefficients is neglected in vibration analysis of crankshaft. Obviously, one reason for this is the numerical methodology, which takes hours of execution time, and no reliable closed-form solutions are available in literature. This paper provides a conceptually simple and rapid means for calculating the stiffness and damping coefficients at each time step.

The stiffness and damping coefficients of oil films do not explicitly appear in the governing equation of non-linear system analysis. The dynamic coefficients can be determined by using Reynolds equation with a first order pressure perturbation (Lund and Thomson, 1978). This gives five equations, one for pressure and other four for partial derivatives of pressure with respect to rotor displacement and velocity components. The journal velocities and displacements can be determined by solving first equation (Reynolds equation without perturbation) with equations of motion by using authors' (Hirani *et al.*, 1998), or any other (Booker, 1971; Ritchie, 1975) technique. In the present study remaining four equations (Reynolds equation for pressure with perturbation of displacement and velocity components) are solved for short and long bearing approximations. The pressure derivatives for finite bearing are determined by taking harmonic average of short and long bearing pressure derivatives. The integration of these pressure derivatives along the axial direction is carried out analytically and Weddle's numerical integration formula is employed in circumferential direction.

Most of the engine bearing analyses are based on the isothermal simplification. However, thermal considerations do play an important role in the engine bearing dynamics. For a given load the thermal effects modify the value of relative eccentricity that leads to a large change in dimensional stiffness and damping coefficients. A complete thermal analysis requires simultaneous solution of generalised Reynolds equation, energy and heat transfer equations with proper boundary conditions (Paranjpe, 1996), which is referred as thermohydrodynamic (THD) analysis. The THD analysis gives probable realistic solution but is computationally intensive and requires a significant amount of time and effort in development. In the present study a simplified thermal analysis is used which is rapid and provides reasonable predictions of the performance.

2. THEORY

The co-ordinate system for a complete (360°) journal bearing operating under extremely general dynamic condition is defined in Fig. 1. For a journal bearing the following assumptions are normally made: body forces are negligible, pressure variation across the film thickness is ignored, the bearing

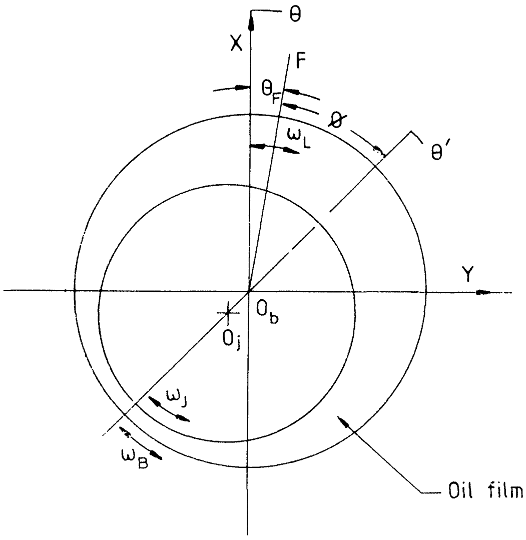

FIGURE 1 Journal bearing.

surface curvature is large compared to film thickness, no slip condition at fluid/bearing surfaces, the lubricant viscosity and density are constant. The Reynolds equation with these assumptions is given as:

$$\frac{1}{R^2}\frac{\partial}{\partial \theta}\left(h^3\frac{\partial P}{\partial \theta}\right) + h^3\frac{\partial^2 P}{\partial z^2} = 6\mu\left(\omega\frac{\partial h}{\partial \theta} + 2\frac{\partial h}{\partial t}\right). \quad (1)$$

In a dynamically loaded journal bearing, the bearing is subjected to variable loads and speeds. In such a situation, a forced motion takes place, consequently generated pressure profile in oil film varies considerably with load fluctuation, and Eq. (1) is required to be solved in a series of time steps. Under such conditions, determination of dynamic coefficients at a static equilibrium position gives unrealistic predictions. The realistic results can be obtained by repeated calculations for dynamic coefficients at each time interval along the locus of the journal centre. This can be achieved by assuming the first order pressure perturbation at each time step, namely:

$$P = P' + P_x\Delta x + P_y\Delta y + P_{\dot{x}}\Delta\dot{x} + P_{\dot{y}}\Delta\dot{y}. \quad (2)$$

Similarly, the film thickness:

$$\begin{aligned} h &= h' + \Delta x\cos\theta + \Delta y\sin\theta, \\ h' &= C(1 + \varepsilon\cos\theta'). \end{aligned} \quad (3)$$

Substituting Eqs. (2) and (3) in Eq. (1), retaining only first order terms, and separating out like terms yields:

$$\begin{aligned} O(1) \Rightarrow \frac{1}{R^2}\frac{\partial}{\partial\theta}\left(h'^3\frac{\partial P'}{\partial\theta}\right) + h'^3\frac{\partial^2 P'}{\partial z^2} \\ = 6\mu\left(\omega\frac{\partial h'}{\partial\theta} + 2\frac{\partial h'}{\partial t}\right), \end{aligned} \quad (4)$$

$$\begin{aligned} O(\Delta x) \Rightarrow \frac{1}{R^2}\frac{\partial}{\partial\theta}\left(h'^3\frac{\partial P_x}{\partial\theta}\right) + h'^3\frac{\partial^2 P_x}{\partial z^2} \\ = -6\mu\omega\sin\theta - \frac{\partial}{\partial\theta}\left(\frac{3h'^2}{R^2}\cos\theta\frac{\partial P'}{\partial\theta}\right) \\ - 3h'^2\cos\theta\frac{\partial^2 P'}{\partial z^2}, \end{aligned} \quad (5)$$

$$\begin{aligned} O(\Delta y) \Rightarrow \frac{1}{R^2}\frac{\partial}{\partial\theta}\left(h'^3\frac{\partial P_y}{\partial\theta}\right) + h'^3\frac{\partial^2 P_y}{\partial z^2} \\ = 6\mu\omega\cos\theta - \frac{\partial}{\partial\theta}\left(\frac{3h'^2}{R^2}\sin\theta\frac{\partial P'}{\partial\theta}\right) \\ - 3h'^2\sin\theta\frac{\partial^2 P'}{\partial z^2}, \end{aligned} \quad (6)$$

$$\begin{aligned} O(\Delta\dot{x}) \Rightarrow \frac{1}{R^2}\frac{\partial}{\partial\theta}\left(h'^3\frac{\partial P_{\dot{x}}}{\partial\theta}\right) + h'^3\frac{\partial^2 P_{\dot{x}}}{\partial z^2} \\ = 12\mu\cos\theta, \end{aligned} \quad (7)$$

$$\begin{aligned} O(\Delta\dot{y}) \Rightarrow \frac{1}{R^2}\frac{\partial}{\partial\theta}\left(h'^3\frac{\partial P_{\dot{y}}}{\partial\theta}\right) + h'^3\frac{\partial^2 P_{\dot{y}}}{\partial z^2} \\ = 12\mu\sin\theta. \end{aligned} \quad (8)$$

The journal velocities and displacements at a particular instant (where external force can be assumed constant) can be evaluated by solving Eq. (4) along with equations of motion by using technique mentioned in (Hirani *et al.*, 1998).

For known rotor centre displacement and velocity components, the stiffness and damping coefficients can be obtained by solving Eqs. (5)–(8).

In this study a new approach is presented for evaluation of dynamic coefficients. This technique requires solutions for short and long bearing approximations. The short bearing approximation, which is commonly used (Hattori, 1993) in practice, neglects the oil film pressure gradients in the circumferential (θ) direction, and the partial derivatives of pressure with respect to displacement and velocity components can be derived for short bearing as:

$$P_{x_o} = \frac{3\mu L^2}{h'^3} \times \left[\omega\sin\theta + \frac{6\cos\theta\left(\dot{\varepsilon}\cos\theta' + \varepsilon(\dot{\phi}-0.5\omega)\sin\theta'\right)}{(1+\varepsilon\cos\theta')}\right] \times \left(\frac{1}{4} - \left(\frac{z}{L}\right)^2\right), \tag{9}$$

$$P_{y_o} = -\frac{3\mu L^2}{h'^3} \times \left[\omega\cos\theta - \frac{6\sin\theta\left(\dot{\varepsilon}\cos\theta' + \varepsilon(\dot{\phi}-0.5\omega)\sin\theta'\right)}{(1+\varepsilon\cos\theta')}\right] \times \left(\frac{1}{4} - \left(\frac{z}{L}\right)^2\right), \tag{10}$$

$$P_{\dot{x}_o} = -\frac{6\mu L^2\cos\theta}{h'^3}\left(\frac{1}{4} - \left(\frac{z}{L}\right)^2\right), \tag{11}$$

$$P_{\dot{y}_o} = -\frac{6\mu L^2\sin\theta}{h'^3}\left(\frac{1}{4} - \left(\frac{z}{L}\right)^2\right). \tag{12}$$

Similarly, the partial derivatives (P_x, P_y, $P_{\dot{x}}$, and $P_{\dot{y}}$) for long bearing approximation can be derived from Eqs. (5)–(8) by ignoring the terms representing variation in axial direction:

$$P_{xs} = \frac{6\mu R^2}{C^3}\left[\begin{array}{c} \dfrac{\omega\sin\phi'}{2\varepsilon}\left(1-\dfrac{1}{H'^2}\right) - \dfrac{\varepsilon(\dot{\phi}-0.5\omega)\sin\phi'}{H'^3}\left(\dfrac{6(1-H'^3)}{(2+\varepsilon^2)} + \dfrac{(3H'-2-H'^3)}{\varepsilon^2}\right) - \dfrac{\dot{\varepsilon}}{\varepsilon^2}\cos\phi' \\ \left(\dfrac{3H'-2}{H'^3}-1\right) + \dfrac{2\dot{\varepsilon}\sin\theta'\sin\phi'}{\varepsilon H'^2}\left(\dfrac{1}{H'} - \dfrac{(1+H')}{(2+\varepsilon^2)}\right) + \dfrac{2\varepsilon(\dot{\phi}-0.5\omega)\sin\theta'\cos\phi'}{\varepsilon H'^2(2+\varepsilon^2)} \\ \left(-\dfrac{2}{H'} + \dfrac{(2+3\varepsilon^2)(1+H')}{(2+\varepsilon^2)}\right) + \dfrac{\omega\sin\theta'\cos\phi\,(1+H')}{(2+\varepsilon^2)\quad H'^2} \end{array}\right], \tag{13}$$

$$P_{ys} = \frac{6\mu R^2}{C^3}\left[\begin{array}{c} \dfrac{\omega\cos\phi'}{2\varepsilon}\left(\dfrac{1}{H'^2}-1\right) + \dfrac{\varepsilon(\dot{\phi}-0.5\omega)\cos\phi'}{H'^3}\left(\dfrac{6(1-H'^3)}{(2+\varepsilon^2)} + \dfrac{(3H'-2-H'^3)}{\varepsilon^2}\right) - \dfrac{\dot{\varepsilon}}{\varepsilon^2}\sin\phi' \\ \left(\dfrac{3H'-2}{H'^3}-1\right) - \dfrac{2\dot{\varepsilon}\sin\theta'\cos\phi'}{\varepsilon H'^2}\left(\dfrac{1}{H'} - \dfrac{(1+H')}{(2+\varepsilon^2)}\right) + \dfrac{2\varepsilon(\dot{\phi}-0.5\omega)\sin\theta'\sin\phi'}{\varepsilon H'^2(2+\varepsilon^2)} \\ \left(-\dfrac{2}{H'} + \dfrac{(2+3\varepsilon^2)(1+H')}{(2+\varepsilon^2)}\right) + \dfrac{\omega\sin\theta'\sin\phi'\,(1+H')}{(2+\varepsilon^2)\quad H'^2} \end{array}\right], \tag{14}$$

$$P_{\dot{x}s} = -\frac{6\mu R^2}{C^3}\left(\frac{2+\varepsilon\cos\theta'}{(1+\varepsilon\cos\theta')^2}\right)\cos\theta, \tag{15}$$

$$P_{\dot{y}s} = -\frac{6\mu R^2}{C^3}\left(\frac{2+\varepsilon\cos\theta'}{(1+\varepsilon\cos\theta')^2}\right)\sin\theta. \tag{16}$$

The analytical expressions for pressure derivatives given in Eqs. (9)–(12) are valid for very short bearing at low load and expressions in Eqs. (13)–(16) are suitable for long bearing at high eccentricity ratio. Hence, both the short and long bearing approximations have limited applications. In present study, pressure derivative's expressions for finite bearing are derived by combining harmonically the short and long bearing solutions:

$$P_n(n = x, y, \dot{x}, \dot{y}) = \frac{P_{n_o}}{1 + |P_{n_o}/P_{ns}|}.$$

This can be re-written as:

$$P_n = \frac{A_n\Big((1/4) - (z/L)^2\Big)}{1 + (1/B_n)\Big((1/4) - (z/L)^2\Big)}, \tag{17}$$

where

$$A_n = P_{n_o}\Big/\Big((1/4) - (z/L)^2\Big),\ B_n = |P_{ns}/A_n|.$$

The stiffness and damping coefficients can be determined by integrating Eq. (17) over bearing surface area. The analytical integration of Eq. (17) with respect to z can be given as:

$$I_{Z_n} = \int_{-L/2}^{L/2} P_n\,\mathrm{d}z = A_nB_nL\left[\int_{-0.5}^{0.5} \frac{(0.25 - \bar{z}^2)}{B_n + 0.25 - \bar{z}^2}\mathrm{d}\bar{z}\right],$$

where $\bar{z} = z/L$, or

$$I_{Z_n} = A_nB_nL\left[1 - \frac{B_n}{\sqrt{B_n + 0.25}} \times \log\left(\frac{\sqrt{B_n + 0.25} + 0.5}{\sqrt{B_n + 0.25} - 0.5}\right)\right].$$

The stiffness and damping coefficients can be presented as:

$$\begin{Bmatrix} K_{nx} \\ K_{ny} \end{Bmatrix} = -\int_{\theta_1}^{\theta_2} I_{Z_n(n=x,y)}\begin{Bmatrix} \cos\theta \\ \sin\theta \end{Bmatrix}\mathrm{d}\theta,$$
$$\begin{Bmatrix} B_{nx} \\ B_{ny} \end{Bmatrix} = -\int_{\theta_1}^{\theta_2} I_{Z_n(n=\dot{x},\dot{y})}\begin{Bmatrix} \cos\theta \\ \sin\theta \end{Bmatrix}\mathrm{d}\theta.$$

The integrations with respect to θ can be determined by using Weddle's integration formula.

3. THERMAL ANALYSIS

The mechanical friction losses in an engine journal bearing are due to shearing of the oil film and generation of pressure due to hydrodynamic and squeezing actions. These losses, appear as heat, raise the temperature of the lubricant within the clearance space, lower its operating viscosity, increase relative eccentricity and therefore affect the dynamic coefficients.

The instantaneous mechanical power loss in a lubricant film arises chiefly from rotational and translational velocities of the journal relative to the bearing and to some extent by pressure generation in film. The shear and squeeze power loss can be given as:

$$H_{\mathrm{Shear}} = \frac{\mu\omega^2LR^3}{C}\left[\int_{\theta_1}^{\theta_2} \frac{1}{(1 + \varepsilon\cos\theta')}\mathrm{d}\theta + (1 - \varepsilon\cos\theta_1)\int_{\theta_1+\pi}^{\theta_2+\pi} \frac{1}{(1 + \varepsilon\cos\theta')^2}\mathrm{d}\theta\right],$$

$$H_{\mathrm{Squeeze}} = C(\dot{\varepsilon}(F_x\cos(\theta_{\mathrm{F}} + \phi) + F_y\sin(\theta_{\mathrm{F}} + \phi)) + \varepsilon(\dot{\phi} - 0.5\omega)(-F_x\sin(\theta_{\mathrm{F}} + \phi) + F_y\cos(\theta_{\mathrm{F}} + \phi))),$$

and total power loss:

$$\mathit{Power\ loss} = |H_{\mathrm{Shear}}| + |H_{\mathrm{Squeeze}}|.$$

A major portion of generated heat is dissipated through the lubricant (convection) and transmitted by the lubricated surfaces (conduction). For simplicity either the heat conducted is neglected (Barwell and Lingard, 1980), or convection as a known portion of total generated heat is considered in energy balance equation. In the second case, which is more realistic, energy balance is given as:

$$\mathit{Oil\ Mass\ Flow\ rate} \times \mathit{Heat\ Capacity\ of\ oil} \times \mathit{Temperature\ rise} = \mathit{Power\ loss} \times \sigma, \tag{18}$$

where, σ is the fraction of the total heat generated, and carried away by the lubricant. A number of related theoretical works have indicated that for lightly loaded bearing this fraction is about 0.5, for moderately loaded it should be $\frac{2}{3}$ to 0.8, and recently Paranjpe (1996) used a value of σ equal to 0.9 for heavily loaded bearings. The authors have suggested a value of σ equal to eccentricity ratio

(Hirani, 1997) and validated this assumption for steadily loaded bearing by obtaining a more realistic prediction by this assumption (Hirani *et al.*, 1997).

The oil flow Q, from an engine bearing involves the hydrodynamic flow Q_H caused by the shaft rotation and the film pressure gradient, together with the feed pressure flow Q_P, which is the direct result of oil being forced through the bearing by supply pressure. Martin (1993) provided suitable combinations of Q_H and Q_P for various feeding arrangements. In the present analysis the axial flow Q is determined by using same formulations as in (Martin, 1993).

The effective temperature rise can be determined by using energy balance, Eq. (18). The effective viscosity can be calculated by using temperature–viscosity relation. Here Walther's temperature–viscosity relation is used.

4. RESULTS AND DISCUSSION

To validate the proposed approximate model for stiffness and damping coefficients, results obtained by using the present study for steadily loaded bearings ($\dot{\varepsilon} = 0$, $\dot{\phi} = 0$) with L/D ratio equal to 0.5 and 1.0, are compared with the results obtained by numerical results (Lund and Thomson, 1978). Figures 2–5 show comparison for non-dimensional stiffness (CK_{nn}/load) and damping ($C\omega B_{nn}$/load), which indicates matching in trend and close agreement in the magnitude of the coefficients.

In order to illustrate the application of proposed methodology to dynamically loaded journal

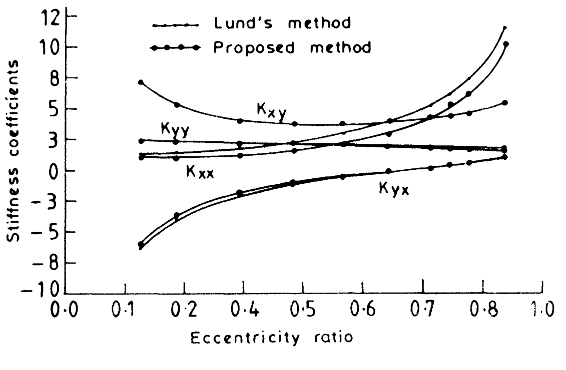

FIGURE 2 Comparison of stiffness coefficients ($L/D = 0.5$).

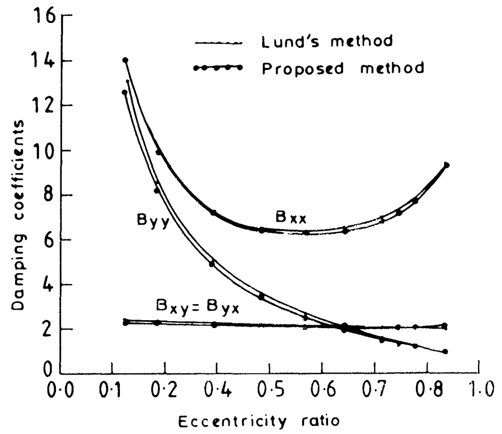

FIGURE 3 Comparison of damping coefficients ($L/D = 0.5$).

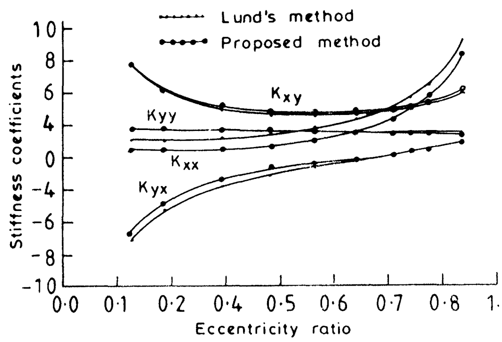

FIGURE 4 Non-dimensional stiffness coefficients ($L/D = 1.0$).

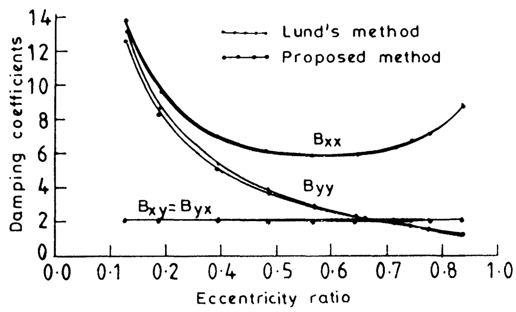

FIGURE 5 Non-dimensional damping coefficients ($L/D = 1.0$).

bearing, two engine bearings (a connecting rod and a main bearing) are analysed. The connecting rod bearing for VEB diesel engine is studied in Example 1, and a main crankshaft bearing for a typical engine (Paranjpe, 1996) is examined in Example 2.

Example 1

To study the variation in stiffness and damping coefficients, the Ruston and Hornsby 6 VEB-X Mk III big end connecting rod is investigated. The rectangular components of bearing load are shown in Fig. 6. The engine and bearing data are as follows: connecting rod length = 0.782 m, crank length = 0.184 m, $C = 82.55\,\mu\text{m}$, $D = 0.2032\,\text{m}$, $L = 0.057\,\text{m}$, $\mu = 0.015\,\text{Pa}\cdot\text{s}$, $\omega_J = -20\pi\,\text{rad/s}$.

The predicted journal locus for this bearing by using a rapid method (Hirani *et al.*, 1998) is given in Fig. 7. The stiffness and damping coefficients are evaluated by proposed scheme, mentioned in Section 2. Figures 8 and 9 show variation in the stiffness and damping coefficients over a crankshaft cycle. Table I indicates that there is large difference in maximum/minimum value compared to mean value. Accordingly it can be concluded that the mean value of these coefficients gives unrealistic results and it is suggested that the variation of these coefficients should be considered in engine vibration studies. The present analysis contains analytical pressure gradients, which reduce time-consuming iterations, and make determination of dynamic coefficients easy.

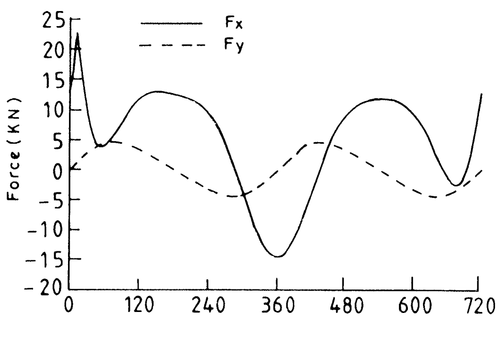

FIGURE 6 Force components.

In the present analysis, unbalance rotor mass is not considered because of unavailability of data. Normally force due to unbalance mass is negligible compared to large engine bearing load, so results will not alter much. The unbalanced mass force can

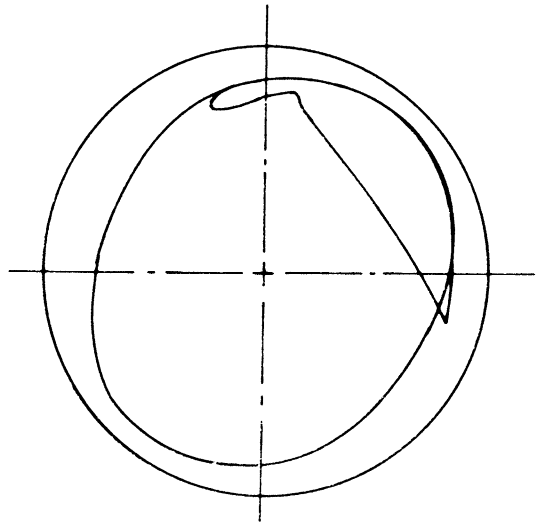

FIGURE 7 Journal orbit in clearance circle (VEB bearing).

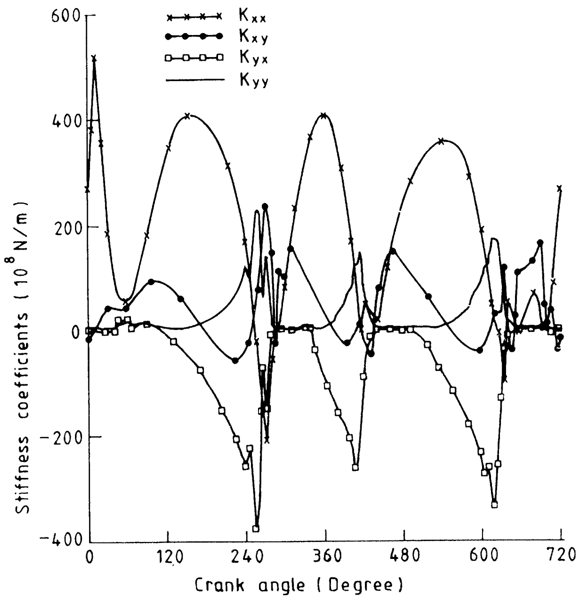

FIGURE 8 Variation of stiffness coefficients over a crankshaft cycle (VEB bearing).

be however included easily. The rotor acceleration can be approximated by Newton's backward difference method, and inertia force can be included in the equations of motion.

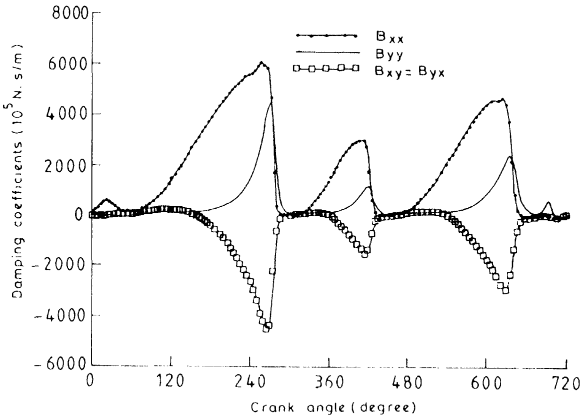

FIGURE 9 Variation of damping coefficients.

Example 2

A typical automotive crankshaft main bearing is analysed to illustrate the application of suggested thermal analysis. The load data are given in Table II. The bearing and lubricant data are as follows: $C = 36\,\mu\text{m}$, $L = 0.021$ m, $R = 0.036$ m, $P_S = 3.5 \times 10^5$ Pa, $T_{in} = 100°\text{C}$, $\omega_J = 523.6$ rad/s, $\mu_{in} = 0.0098$ Pa · s, $\rho_o = 840\,\text{kg/m}^3$, $C_O = 2083$ J/kg °C, groove extent = 20–180°, groove width = 0.0042 m.

TABLE I Maximum, average and minimum values of dynamic coefficients over a crankshaft cycle

Dynamic coefficients	Maximum	Average	Minimum
K_{xx} ($\times 10^8$)	520	208	−2.07
K_{xy} ($\times 10^8$)	236	443	−59.1
K_{yx} ($\times 10^8$)	24.1	−7.1	−3.73
K_{yy} ($\times 10^8$)	225	3.25	1.72
B_{xx} ($\times 10^5$)	6128	187.6	7.33
$B_{xy} = B_{yx}$ ($\times 10^5$)	249	−52.7	−4533
B_{yy} ($\times 10^5$)	4477	50.7	14.9

TABLE II Main bearing loads at 5000 rpm

Angle (Deg)	F_x (N)	F_y (N)	Angle (Deg)	F_x (N)	F_y (N)	Angle (Deg)	F_x (N)	F_y (N)
0	3396	−4062	250	3074	−24329	500	7037	−2520
10	7003	−7750	260	3433	−22971	510	5599	−2755
20	8287	−7567	270	504	−16973	520	4011	−2979
30	7476	−4726	280	−1556	−12316	530	2329	−3217
40	7169	−2926	290	−2733	−8884	540	787	−3132
50	7379	−2060	300	−2745	−5530	550	−734	−3059
60	7890	−1909	310	−2280	−2877	560	−2412	−3284
70	8434	−2307	320	−2119	−1591	570	−4029	−3441
80	8739	−3198	330	−1975	−810	580	−5520	−3516
90	8586	−4604	340	−1914	−520	590	−6833	−3466
100	7894	−6531	350	−1827	−566	600	−7901	−3257
110	6899	−8611	360	−3031	−3331	610	−8634	−2923
120	2195	−16901	370	−3707	−6218	620	−8961	−2485
130	−1783	−24879	380	−2554	−6451	630	−8872	−1934
140	−1967	−25561	390	−228	−4506	640	−8385	−1298
150	−71	−20288	400	1926	−3206	650	−7561	−608
160	655	−16297	410	3940	−2529	660	−6489	57
170	478	−13672	420	5367	−1559	670	−5273	601
180	−509	−11663	430	6649	−840	680	−3993	929
190	−1711	−10449	440	8056	−1018	690	−2683	929
200	−2699	−10360	450	9046	−1271	700	−1336	562
210	−3508	−10859	460	9554	−1547	710	−13	44
220	−4019	−11806	470	9559	−1823	720	3396	−4062
230	−4258	−12725	480	9104	−2068			
240	−865	−19057	490	8240	−2285			

In the present analysis, the properties of typical SAE 30 oil are used for thermal analysis. The Walther's viscosity–temperature relation is used, to represent the viscosity variation of this oil with temperature as follows:

$$\mu = \rho_0 \left[10^{10^{(8.8813-3.4389)\times\log(T)}} - 0.6 \right].$$

The journal orbit for journal of the main bearing obtained by using isothermal (Hirani *et al.*, 1998), and thermal analysis is given in Fig. 10. The simplified thermal analysis follows same trend as isothermal case, but gives better prediction of eccentricity ratio. The temperature effects increase eccentricity ratio, which is seen in Fig. 10.

Figures 11–14 show variation of stiffness and damping coefficients for thermal and isothermal (constant viscosity) case. Five to ten percent variations in dynamic coefficients between isothermal and thermal analysis can be visualised from these figures. The required computing time for presented simple thermal analysis is comparable to that taken by isothermal analysis, and it gives realistic results compared to isothermal analysis. Accordingly, one can recommend the thermal analysis for simulation of stiffness and dynamic coefficients.

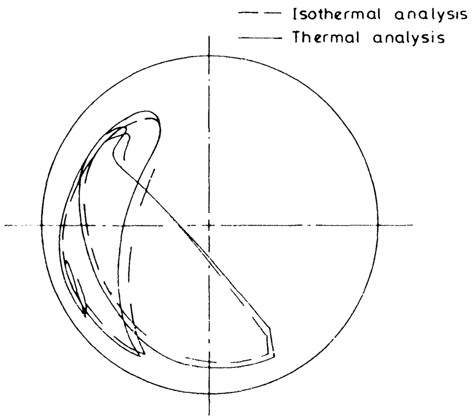

FIGURE 10 Journal orbit for thermal and isothermal analysis.

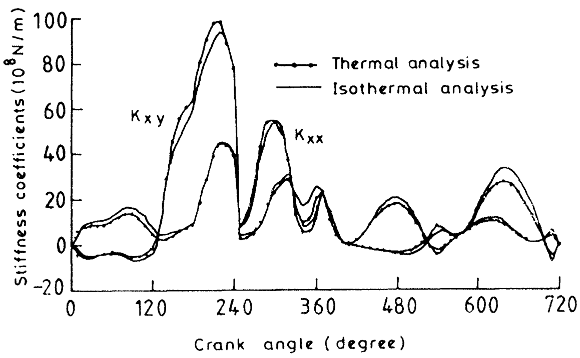

FIGURE 11 Stiffness coefficients (K_{xx} and K_{xy}) for thermal and isothermal analysis.

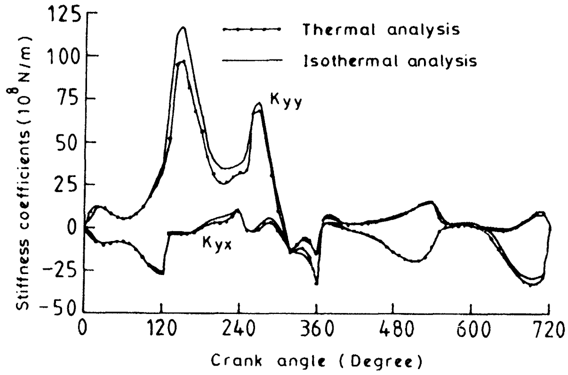

FIGURE 12 Variation of stiffness coefficients for thermal and isothermal analysis.

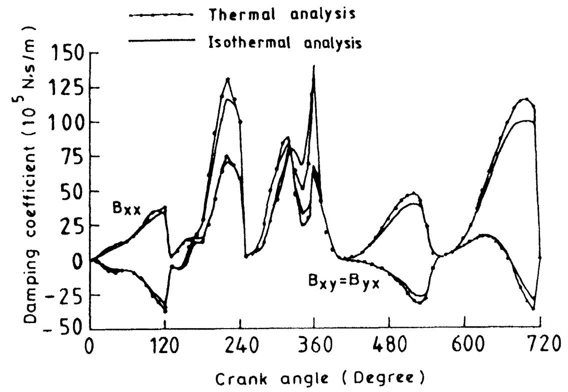

FIGURE 13 Comparison of damping coefficients for isothermal and thermal analysis.

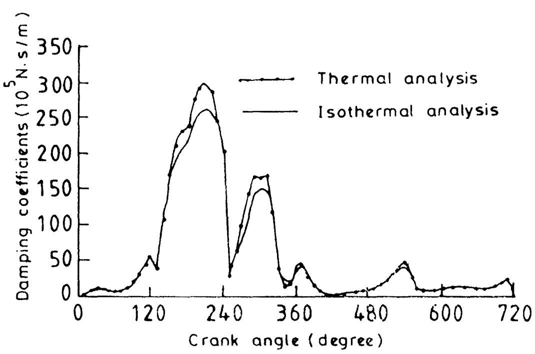

FIGURE 14 Variation in B_{yy} for isothermal and thermal analysis.

Acknowledgements

We express our thanks to Dr. Rohit Paranjpe, Engine Research Department, R&D Centre, General Motors Corporation, USA, for providing the main bearing data (Table II). We are also thankful to Mr. T.V.V.L.N. Rao, a research student for allowing us to use his computer program based on Lund's finite-difference technique (Lund and Thomson, 1978) for comparison (Figs. 2–5) with the present study.

NOMENCLATURE

$B_{xx}, B_{xy}, B_{yx}, B_{yy}$	damping coefficients, N s/m
C	radial clearance, m
C_O	specific heat of lubricant, J/kg °C
D	journal diameter, m
F, F_x, F_y	bearing force, N
h	film thickness, m
H'	non-dimensional film thickness, $(1+\varepsilon\cos\theta')$
H_{Shear}	power loss due to rotation, W
H_{Squeeze}	power loss due to squeeze, W
$K_{xx}, K_{xy}, K_{yx}, K_{yy}$	stiffness coefficients, N/m
L	bearing length, m
P	dimensional pressure, N/m^2
P_S	supply pressure, N/m^2
Q_H, Q_P	side leakage due to hydrodynamic action and feed pressure, m^3/s
R	journal radius, m
t	time, s
T_{in}, T_{eff}	inlet and effective temperature, °K
z	axial co-ordinate, m
ΔT	global temperature rise, °K
Λ	slenderness ratio, L/D
ε	eccentricity ratio
ϕ	attitude angle
μ	dynamic oil viscosity, Pa · s
θ	co-ordinate in circumferential direction, rad
ρ_o	density of lubricant, kg/m^3
ω_J	angular speed of journal, rad/s
ω	angular speed of rotation, rad/s

References

Barwell, F.T. and Lingard, S., 1980, Thermal equilibrium of plain journal bearings, *Thermal Effects in Tribology*, *Proceedings of the 6th Leeds-Lyon symposium on Tribology*, Eds. D. Dowson, C.M. Taylor, M. Godet and Berthe, pp. 24–32, Institut National des Sciences Appliques de Lyon, France.

Booker, J.F., 1971, Dynamically loaded journal bearing: numerical application of the mobility method, *Trans. ASME, Journal of lubrication Technology*, **93**, 168–176.

Goenka, P.K., 1984, Dynamically loaded journal bearings: finite element method analysis, *Trans. ASME*, *Journal of Lubrication Technology*, **106**, 429–439.

Hattori, H., 1993, Dynamic analysis of a rotor-journal bearing system with large dynamic loads, *JSME International Journal, Series C*, **36**, 251–257.

Hirani, H., 1997, "Dynamically loaded journal bearings", *Proc. on Lubrication*: *Key to Bearing Survival*, Eds. K.N. Mistry and A.K. Dave, pp. 10.1–10.22, S.V.R.E.T. Surat (India).

Hirani, H., Rao, T.V.V.L.N., Athre, K. and Biswas, S., 1997, Rapid performance evaluation of journal bearings, *Tribology International*, **30**(11), 825–834.

Hirani, H., Athre, K. and Biswas, S., 1998, Rapid and globally convergent method for dynamically loaded journal bearing design, *Proc. IMechE, Part J, Journal of Engineering Tribology*, **212**, 207–214.

Lund, J.W. and Thomson, K.K., 1978, A calculation method and data for the dynamic coefficients of oil lubricated journal bearings, *Topic in Fluid Bearing and Rotor Bearing System*, ASME, New York, pp. 1–28.

Martin, F.A., 1993, Engine bearing design: Design studies, wider aspects and future development, *Engine Tribology*, Elsevier Science Publisher, pp. 113–157.

Paranjpe, R.S., 1996, A study of dynamically loaded engine bearings using a transient thermohydrodynamic analysis, *Tribology Transactions*, **39**, 636–644.

Parszewski, Z.A. and Krynicki, K., 1989, Rotor–bearing system stability: composition approach with bearing shape function presentation, *Tribology Transactions*, **32**, 517–523.

Ritchie, G.S., 1975, The prediction of journal loci in dynamically loaded internal combustion engine bearings, *Wear*, **135**, 291–297.

Roshan, P., Sinhasan, R. and Singh, D.V., 1987, Analysis of a big-end bearing – A finite element approach, *Wear*, **114**, 275–293.